Thermoreversible Gelation of Solutions of Syndiotactic Poly(methyl methacrylate) in Toluene: A Two-Step Mechanism

M. Berghmans, S. Thijs, M. Cornette, H. Berghmans,* and F. C. De Schryver*

Department of Chemistry, Katholieke Universiteit Leuven, Celestijnenlaan, 200F B-3001 Leuven, Belgium

P. Moldenaers and J. Mewis

Department of Chemical Engineering, Katholieke Universiteit Leuven, de Croylaan, 46 B-3001 Leuven, Belgium

Received July 1, 1994; Revised Manuscript Received September 22, 1994

ABSTRACT: The thermoreversible gelation of solutions of syndiotactic poly(methyl methacrylate) in toluene has been studied by different experimental techniques. A combination of calorimetric, infrared, fluorescence, light scattering, and rheological observations supports the two-step gelation mechanism, proposed in a previous paper. A fast intramolecular conformational change is followed by an intermolecular association. The change in molecular mobility during the gelation process has been followed by ^{1}H NMR. Further support for the two-step mechanism has been found in the temperature dependence of the fluorescence properties of a probe covalently attached to the polymer chain. Finally, a concentration–temperature diagram for the polymer–solvent system has been constructed.

Introduction

The solution behavior of syndiotactic poly(methyl methacrylate) (sPMMA) has been studied extensively by different authors using a wide variety of experimental techniques. The crystallization of this polymer from the melt has never been reported. The formation of a regular, crystalline supramolecular structure is only possible in the presence of a solvent. Most of the data published in the literature are compiled in a recent review article.[1]

The overall tacticity and solvent quality play a major role in the formation of these structures, and this is clearly illustrated by the very different behavior of the polymer in *o*-xylene and butyl acetate. Thermoreversible gels are formed in *o*-xylene[2–7] while floculation and sedimentation take place in butylacetate.[8,9] The important changes in molecular mobility, which accompany this structure formation, were studied by ^{1}H NMR and quantitative information on the degree of association, and the kinetics of the process have been obtained.[5–7,10–12]

The change in molecular conformation was followed by infrared (IR) spectroscopy.[13–15] The two signals of the $-CH_2-$ rocking vibration doublet can be ascribed to two different chain conformations. The absorption at 860 cm^{-1} is characteristic for the all trans or close to the all trans (TT) conformation. Theoretical calculations designate this slightly deformed TT conformation as the energetically most stable on which the helix conformation of the polymer chain is based.[1] The trans-gauche conformation (TG) absorbs at 843 cm^{-1} and is characteristic of the random coil. It is the predominant conformation when sPMMA is dissolved in a good solvent like chloroform. The intensity ratio of these two signals (TT/TG or I_{860}/I_{843}) has been used as a quantitative measure for the degree of coil to helix transformation. The inclusion of the solvent in this helix and its participation in a intermolecular association has been suggested.[16,17]

* Abstract published in *Advance ACS Abstracts,* November 15, 1994.

Table 1. Characteristics of the Different Polymers

sample	$M_w \times 10^{-3}$	$M_n \times 10^{-3}$	M_w/M_n	% syndiotactic triads
sPMMA1	169	91	1.9	90
sPMMA2	233	115	2.0	92
sPMMA3	157	88	1.8	90
sPMMA[a,1]	179	49	3.7	89
sPMMA[a,2]	237	91	2.8	87
aPMMA[a]	159	89	1.78	

[a] Pyrene-labeled PMMA.

Previously, a detailed study of the thermoreversible gelation of solutions of syndiotactic poly(methyl methacrylate) in *o*-xylene has been reported.[18] Moderately concentrated solutions form transparent, thermoreversible gels on cooling. A two-step gelation mechanism was proposed in which the first step consists of an intramolecular coil to helix transition. Intermolecular association takes place in a second step, leading to the formation of a physical network.

In this paper, the data obtained in a similar investigation of solutions of sPMMA in toluene, using a wider range of experimental techniques, will be reported.

Experimental Section

1. Materials. sPMMA was obtained by polymerization of methyl methacrylate (MMA) at −78 °C in toluene with aluminum triethyl and titanium(IV) chloride as the catalyst. This synthesis has been repeated different times, resulting in the formation of polymers with very analogous characteristics. A limited amount of polymer has been obtained in every synthesis, and therefore different samples had to be used throughout this work. The weight and number average molecular weights (respectively, M_w and M_n) have been determined by gel permeation chromatography in tetrahydrofuran. The percentage of syndiotactic triads has been obtained from ^{13}C NMR experiments.[19] The characteristics of the different PMMA samples are reported in Table 1.

1-Pyrenemethyl methacrylate (1-PMA) has been prepared by condensation of methacryloyl chloride with 1-pyrenemethanol in tetrahydrofuran in the presence of pyridine as a base, in analogy with the reported synthesis of the naphthalene derivative.[20]

0024-9297/94/2227-7669$04.50/0

1-Pyrenemethanol has been prepared by reduction of 1-pyrenealdehyde with $LiAlH_4$ in a diethyl ether–tetrahydrofuran mixture (80/20).

1-Pyrenemethyl pivalate (1-PA), a model compound for 1-PMA, has been prepared by reaction of pivaloyl chloride with 1-pyrenemethanol.

The structures of these three low molecular weight compounds have been confirmed by ^1H NMR analysis. The corresponding absorptions, observed in $CDCl_3$, are as follows. For 1-PMA: δ = 1.98, CH_3; 5.5, =CH–; 5.8, CH_2; 6.4, =CH–; 8.1, pyrene. For 1-PA: δ = 1.1, CH_3; 5.8, CH_2; 8.1, pyrene.

Labeled sPMMA (sPMMA*) has been prepared by copolymerization of MMA (0.99) with 1-PMA (0.01). Its characteristics are also reported in Table 1.

2. Experimental Methods. Calorimetric observations have been made with a Perkin-Elmer DSC-2, equipped with a thermal analysis data station. Large volume sample pans, containing around 50 mg of solution, have been used. The scanning rate is 5 °C/min. The concentrations are expressed in mass fraction (w_2) of the polymer (g/g).

NMR observations have been made with a Brucker 250.

IR measurements were performed with a Perkin-Elmer 882 infrared spectrophotometer in sealed liquid cells that can be subjected to controlled temperature changes.

A Perkin-Elmer Lambda 6 UV/VIS spectrophotometer has been used to record the absorption spectra.

Fluorescence spectra have been recorded with a SLM 8000 C spectrofluorimeter exciting at 320 nm. Stationary fluorescence anisotropy measurements were carried out with an SLM-8000C spectrofluorometer in L-format, correcting for polarization bias in the detection system. The temperature, monitored inside the cuvette (quartz, 1-cm) using a RPt100 resistor, was controlled (±0.5 °C) by a Lauda RUL 480 thermostat–cryostat.

Fluorescence decay parameters have been measured with a Spectra Physics frequency-doubled, cavity-dumped, mode-locked, synchronously pumped DCM-dye laser with time correlated single photon timing detection.[21]

Light scattering experiments have been performed with an AMTEC MM 1000 spectrogoniometer with a He–Ne laser as the light source.

Rheological observations have been made with a rheometrics RMS 750. Porous, parallel plates were used. Details about this technique are described elsewhere.[18]

Results and Discussion

1. Intra- and Intermolecular Transitions in Solution. 1.1. Calorimetric Observations. Calorimetric observations provide information on the gelation as a whole. It is an exothermic phenomenon that takes place on cooling. Heating results in the endothermic melting of the gel. An example of the corresponding DSC scans is represented in Figure 1 (w_2 = 0.10). The average enthalpy change of this transition is 19 J g^{-1}. The melting region extends over about 30 °C, and the endotherm shows a maximum at 53 °C. The exothermic signal sets in at 34 °C and reaches a minimum at 27 °C. The hysteresis, defined as the temperature difference between the temperature at the maximum of the melting endotherm and the minimum of the gelation endotherm , is to a large extent due to the thermal inertia of the system. It has been shown for the system sPMMA–*o*-xylene that this hysteresis can be strongly reduced by extrapolation to zero scanning rate.[18]

1.2. Infrared Observations. The change in intramolecular conformation is followed by infrared spectroscopy. The temperature dependence of the intensity of the two absorption peaks of the $-CH_2-$ rocking vibration, mentioned in the introduction, is investigated. Their normalized, equilibrium intensity ratio is plotted as a function of the temperature in Figure 2 (w_2 = 0.10). Its value is a measure of the amount of chain units that

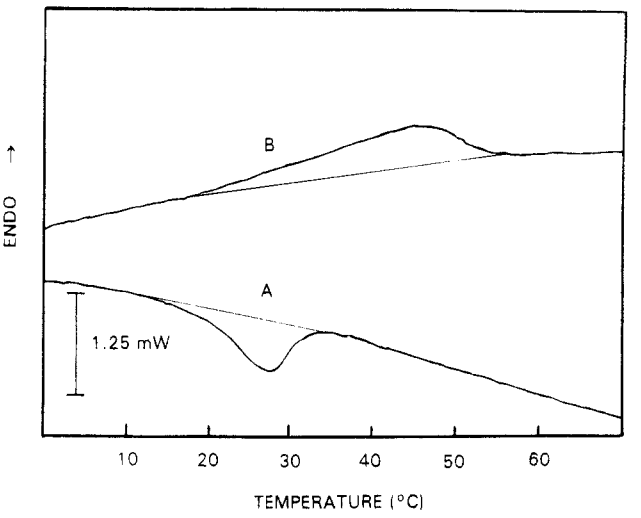

Figure 1. DSC scan of a solution of sPMMA1 in toluene (w_2 = 0.1; A, cooling; B, heating).

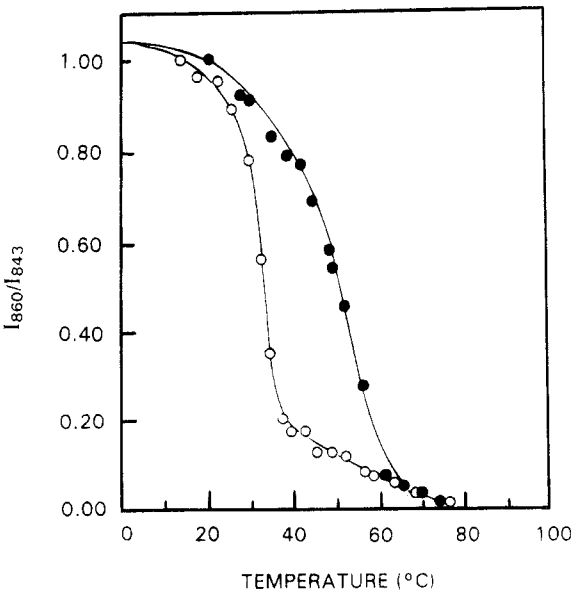

Figure 2. IR intensity ratio I_{860}/I_{843} as a function of temperature (w_2 = 0.1; ○, cooling, ●, heating).

take part in the formation of a regular helix. Its slow, linear increase with decreasing temperature in the high temperature region (T > 60 °C) indicates the increase in population of the energetically most favorable TT conformation in the random coil polymer in solution. A much more pronounced increase is observed at lower temperature. An S-shaped curve, extending up to room temperature, is obtained. This important change is ascribed to the transition from the random coil conformation to the more regular helix conformation. An important hysteresis is observed on heating. It is similar to the one encountered in the calorimetric observations.

1.3. High Resolution Nuclear Magnetic Resonance. A change in molecular conformation from a random coil to a regular helix will reduce the chain mobility. This will result in a decrease of the integrated intensity of the NMR signals of the protons involved in this transition. A degree of rigidification, p, can be calculated using eq 1:[1]

$$p = 1 - I/I_0 \qquad (1)$$

The intensity obtained with a sample that did undergo some molecular change is represented by I, while

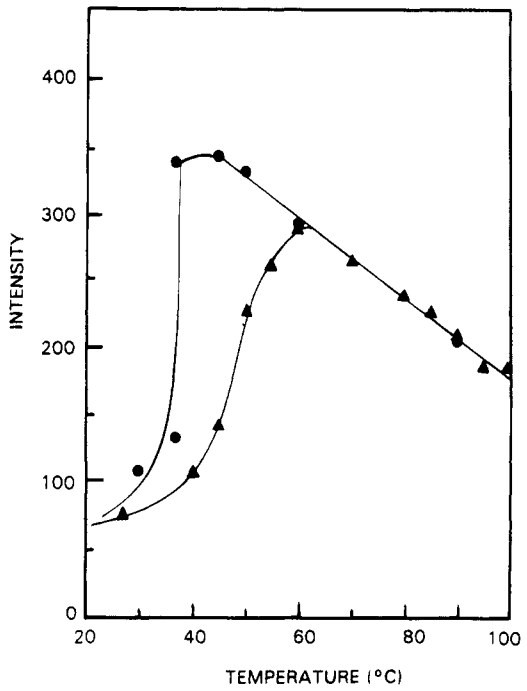

Figure 3. Temperature dependence of the integrated intensity of the 1H NMR spectra (sPMMA2; $w_2 = 0.05$; ●, cooling; ▲, heating).

I_o represents the intensity obtained with a randomly coiled polymer, dissolved in chloroform. The predominance of the random coil conformation in this solvent is supported by the low intensity ratio of the two IR peaks, I_{860}/I_{843}.

The change in mobility of the α-methyl protons has been followed as a function of temperature, and the integrated intensity of the corresponding resonance signal is plotted against the temperature in Figure 3. A linear increase is observed at high temperature ($T >$ 48 °C) according to eq 2 representing the temperature dependence of the peak intensity in absence of any specific structural transition

$$I = KSN(1/T) \qquad (2)$$

where K is a constant taking into account the characteristics of the apparatus, S is the saturation factor, and T represents the absolute temperature. The number of mobile nuclei per unit volume is given by N. A dramatic decrease sets in at 48 °C and extends over a narrow temperature region. The fraction of immobilized protons at 30 °C is 0.84. Heating of the sample restores the original situation. The temperature region in which these changes take place and the extent of the hysteresis are comparable to those observed in DSC and IR.

1.4. Fluorescence measurements. Fluorescence spectroscopy is a technique that offers a wide range of possibilities to study molecular mobility. This was already used previously to study polymer conformation change and thermoreversible gelation.[25,26] Because sPMMA has no intrinsic chromophores, the polymer was labeled in these experiments with a fluorescent molecule.

1.4.1. Fluorescence Characteristics of the Labeled Polymer. sPMMA, containing 1% 1-pyrenemethyl methacrylate as a comonomer, has been synthesized. An average of four labeled monomer units per polymer chain has been calculated from absorption measurements. This copolymerization does not influence the tacticity and the molecular weight of the polymer. A low molecular weight material, 1-pyrene pivalate, has been used as a model.

The fluorescence spectra of the model compound is influenced by the concentration. At high concentrations a broad structureless band appears with a maximum at 485 nm which is ascribed to excimer formation. This band is absent at low concentration. This concentration dependence of the intensity of the excimer formation is not observed with the labeled polymer. In this case the local concentration of chromophores must always be relatively high, and excimer formation is observed at any polymer concentration.

The fluorescence decay of a solution of sPMMA*1 in toluene at 377 nm can be analyzed as a sum of two exponential functions. The longer lived component of the emission can be attributed to chromophores that cannot form an excimer during the excited state lifetime. The shorter lived emission originates from chromophores at excimer-forming sites.[20] This attribution is supported by the analysis of the fluorescence decay at 500 nm.

This kinetic scheme has been further confirmed by using a polymer with a lower concentration of built in chromophores (0.1%). No excimer emission is observed in the fluorescence spectra of a solution of this polymer, and a monoexponential fluorescence decay with a decay time of 212 ns is observed for a gel with $w_2 = 0.05$. This proves that the biexponential fluorescence decay is a consequence of the "intrachain" excimer formation.

The contribution of the excimer emission to the biexponential fluorescence decay is limited because of the low concentration of these chromophores along the polymer chain. Consequently, the longest component in the decay has been used in this study of the gelation. This has been justified by a limited number of experiments using a sPMMA with 0.1% pyrene labels that did not show excimer formation and for which the decay corresponds to this longest decay component.

1.4.2. Study of the change in molecular conformation. The change in chain conformation is studied by measuring the fluorescence decay of the probe at different temperatures. In a first series of experiments a dilute solution with a polymer concentration $w_2 =$ 0.005 has been used. Under these conditions no macroscopic gel is formed. When the solution is cooled, a sharp increase in the decay time, extending over only a few degrees, sets in around 50 °C (Figure 4). This change is situated in the temperature range where the first traces of conformational change are observed by IR. The recorded values represent equilibrium data at each temperature. The recorded value is obtained as soon as the sample reaches the desired temperature, and no further change with time was observed. An increase in the solute concentration ($w_2 = 0.05$) only displaces the onset of this transition to higher temperature without influencing its position as a whole on the temperature scale. This sudden change in decay time is not observed for a solution in toluene of the atactic, labeled PMMA. A linear decrease, also represented in Figure 4, is observed over the whole temperature range studied.

The change in fluorescence characteristics can be related to the change in chain conformation. In a random coil, the chromophores are predominantly surrounded by polar ester groups. This results in a lower fluorescence decay time. The transition from this random coil to a helix conformation of some of the molecular segments will expand the chain molecule. The less polar solvent, toluene, will replace the more polar

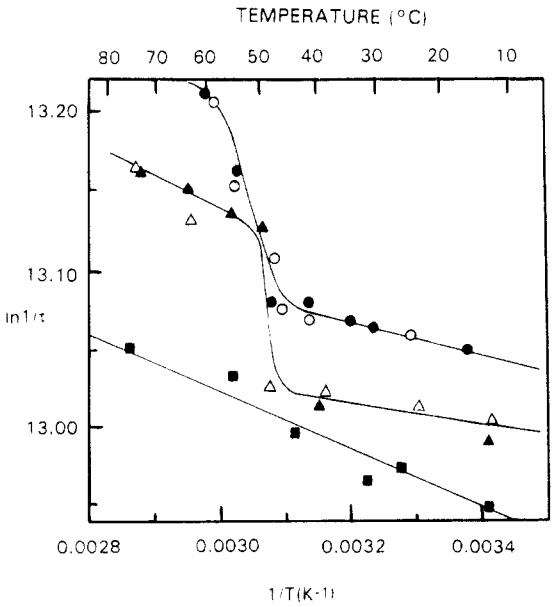

Figure 4. Fluorescence lifetime [τ, plotted as $\ln(1/\tau)$] of the probe as a function of temperature (■, aPMMA*; ▲, sPMMA1* 0.005 g/g heating; △, sPMMA1* 0.005 g/g cooling; ●, sPMMA1* 0.05 g/g heating; △, sPMMA1* 0.05 g/g cooling).

ester groups and the polarity in the vicinity of the chromophore will decrease. This leads to an increase in the fluorescence decay time. This was corrobated by measuring the decay times of 1-pyrenemethyl pivalate in, respectively, toluene and ethyl acetate (results not shown).

The transition of a few segments of the chain from the coil to the helix conformation seems to be sufficient to realize this change in solvation of the pyrene groups. A study of the helix-coil transition of the 1-pyreneacrylic acid–methacrylic acid copolymer as a function of the pH has led to similar conclusions.[22]

1.4.3. Intramolecular Associations. A study of stationary fluorescence anisotropy of the pyrene label provides additional information on the thermal transitions that take place on gelation and gel melting. A solution of sPMMA*1 in toluene with a $w_2 = 0.1$ shows no fluorescence anisotropy at temperatures above the gel temperature. However, upon cooling the solution, fluorescence anisotropy is observed at temperatures below the gelation temperature. The mean value of the fluorescence anisotropy over the interval ranging from 370 nm to 420 nm is plotted as a function of temperature in Figure 5. At low temperature the solution is rigid and the fluorescence of the probe shows anisotropy. The gel melts when reheating, and this results in the disappearance of the physical network and an important decrease in the fluorescence anisotropy in the temperature region in which a transition is observed by IR, DSC, and ^{1}H NMR.

A dilute solution of sPMMA*1 in toluene with a concentration of $w_2 = 0.001$ shows no fluorescence anisotropy, neither do solutions of labeled aPMMA at any concentration in the same temperature region, clearly indicating that network formation and not conformational change leads to this fluorescence anisotropy.

A very large hysteresis, which is a function of the cooling rate, is observed. This is due to the fact that the values for the fluorescence anisotropy in this experiment are not equilibrium values. A plot of the changes in fluorescence anisotropy of a $w_2 = 0.1$ solution in toluene of sPMMA*1 at 35 °C as a function of time

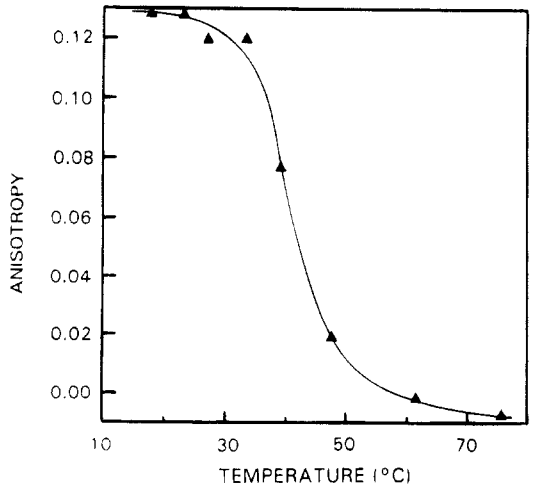

Figure 5. Fluorescence anisotropy as a function of temperature (sPMMA*; $w_2 = 0.1$).

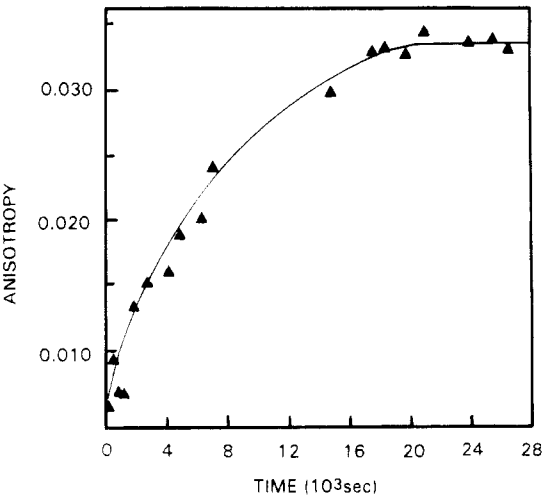

Figure 6. Fluorescence anisotropy as a function of time at 35 °C (sPMMA*; $w_2 = 0.1$).

clearly shows that 5–6 h are needed before equilibrium is reached at that temperature. This is illustrated in Figure 6.

1.5. Light Scattering Observations. Light scattering observations have been carried out with toluene solutions in the low concentration region where macroscopic gel formation is not taking place ($w_2 < 0.01$). At these concentrations, microgel particles are nevertheless formed. Their presence can easily be established by the difficulties encountered in filtering these solutions at room temperature. The change in intensity of the scattered light has been followed as a function of polymer concentration and temperature at a scattering angle of 60°.

In a first series of experiments, a solution in toluene with $w_2 = 0.0046$ is cooled and heated at 10 °C/min. The inverse of the intensity, recorded during these dynamic experiments, is plotted as a function of temperature in Figure 7. When the solution is cooled, the scattered intensity suddenly increases at 35 °C, and a maximum value is reached at 20 °C. An important hysteresis is observed on heating. When the solution is heated the decrease of the scattered intensity sets in at 48 °C.

Equilibrium values of the scattered intensity at a given concentration are obtained from its time dependence at constant temperature. The scattered intensity is followed as a function of time at different temperatures and polymer concentrations until a constant

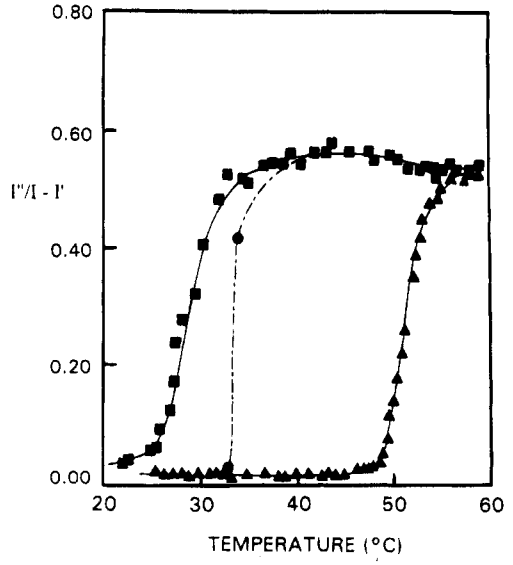

Figure 7. Inverse of the scattered intensity, I [plotted as $I''/(I - I')$], as a function of temperature for a solution of sPMMA3 ($w_2 = 4.6 \times 10^{-3}$; I, solution; I', solvent; I'', benzene reference; ■, cooling; ▲, heating; ●, equilibrium).

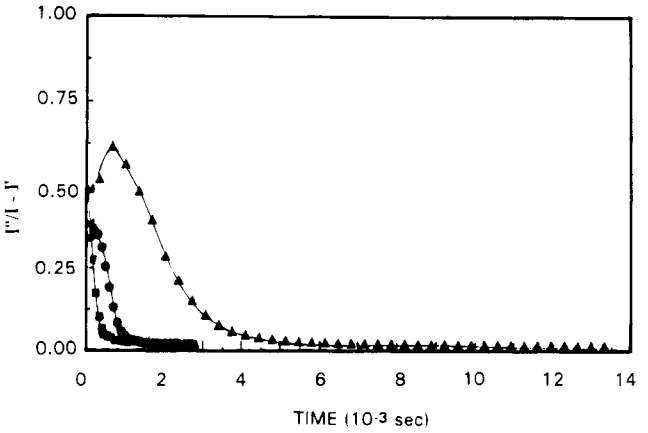

Figure 8. Inverse of the scattered intensity, I [plotted as $I''/(I - I')$], as a function of time at different temperatures for sPMMA 3 ($w_2 = 5.7 \times 10^{-3}$; I, solution; I', solvent; I'', benzene reference; ■, 20 °C; ●, 25 °C; ▲, 30°C).

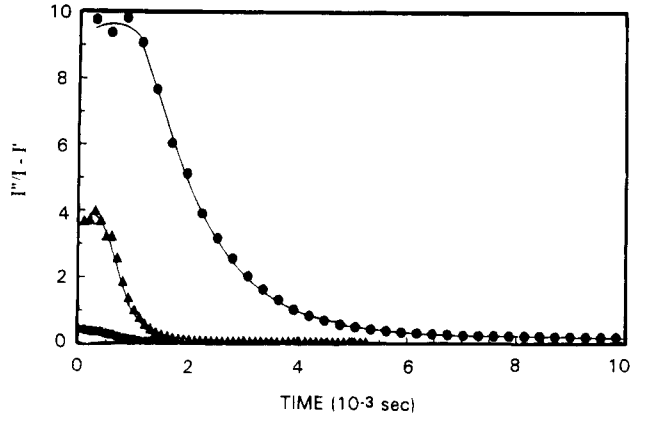

Figure 9. Inverse of the scattered intensity I [plotted as $I''/(I - I')$] as a function of time at different concentrations for sPMMA 3 (●, $w_2 = 6 \times 10^{-4}$; ▲, $w_2 = 3.1 \times 10^{-3}$; ■, $w_2 = 5.7 \times 10^{-3}$; I, solution; I', solvent; I'', benzene reference).

intensity is recorded. Typical intensity–time curves, recorded at different temperatures but constant concentration are given in Figure 8. The change of intensity at constant temperature as a function of concentration of these transitions is represented in Figure 9. These equilibrium data are also transferred to Figure 7. The difference with the data obtained during a dynamic experiment clearly illustrates the time dependence of intermolecular association. Half-life times have been deduced from these kinetic observations. Their concentration and temperature dependence are reported in Table 2.

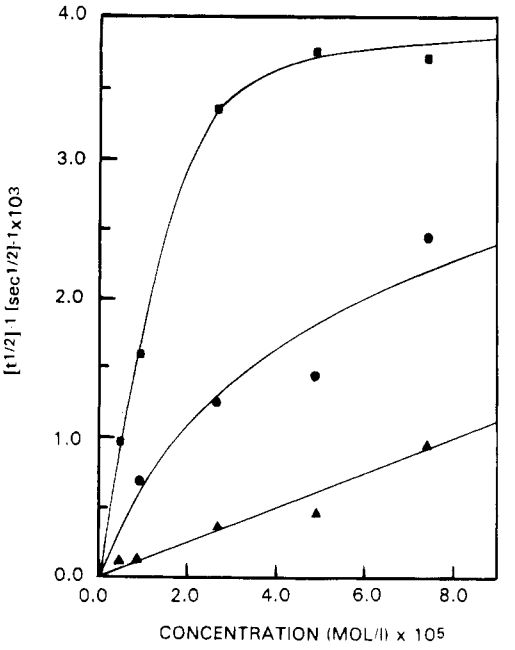

Figure 10. Inverse of the half-life time as a function of concentration at three different temperatures (■, 20 °C; ●, 25°C; ▲, 30°C).

Table 2. Half-life Times as a Function of Concentration at Different Temperatures. The Concentrations Have Been Recalculated in mol/L

concn (w_2)	concn (mol/L)	$t_{1/2}$ 20 °C (s)	$t_{1/2}$ 25 °C (s)	$t_{1/2}$ 30 °C (s)
6.0×10^{-4}	5.20×10^{-6}	1038	1824	8400
1.1×10^{-3}	9.54×10^{-6}	635	1459	8167
3.1×10^{-3}	2.69×10^{-5}	298	806	2750
5.7×10^{-3}	4.95×10^{-5}	266	696	2167
8.6×10^{-3}	7.47×10^{-5}	269	410	1059

The concentration dependence of $t_{1/2}$ can be used in the determination of the order of a reaction. A second-order intermolecular association transition has already been reported for the gelation of sPMMA.[23,24] Therefore, the inverse of $t_{1/2}$ has been plotted as a function of the concentration at different temperatures (Figure 10). A linear plot is only obtained at the highest temperature used in this set of experiments. One could therefore conclude that, at this temperature, where gelation proceeds rather slowly, a second-order association mechanism is responsible for the formation of the scattering elements. At lower temperatures, gelation proceeds much faster and no conclusions about the order of the intermolecular association can be drawn.

1.6. Rheological Observations. Gels formed at room temperature are rigid and transparent. Virtually no syneresis is observed. Their mechanical properties have been investigated by dynamic mechanical experiments. The frequency dependence of G' and G'' have been investigated, and their respective values as a function of frequency are plotted in Figure 11 for a solution with a concentration of $w_2 = 0.10$. At 20 °C, a plateau value of 2.6×10^3 Pa is obtained for G' while the value of G'' is low and increases only slightly with increasing frequency. This elastic gel network supports deformations up to 10% at a frequency of 10 rad/s.

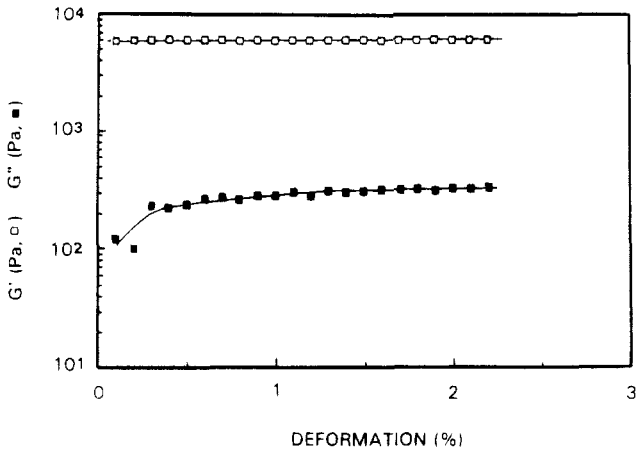

Figure 11. G' and G'' as a function of the degree of deformation at constant frequency (10 rad/s; sPMMA1; $w_2 = 0.1$).

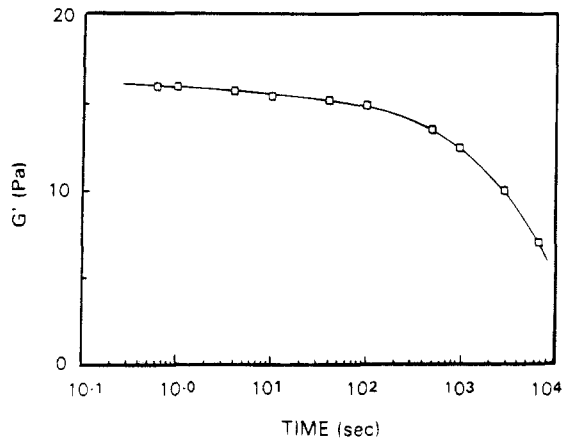

Figure 12. G' as a function of time at constant degree of deformation (0.5%; sPMMA1; $w_2 = 0.10$).

Stress relaxation as a function of time takes place at constant deformation. This is given in Figure 12.

Gelation at room temperature is almost instantaneous, and no time effects can be studied at this temperature. This is only possible at higher temperatures at which only a small fraction of monomer units is incorporated in a regular conformation. Therefore, the change of G', the elastic part of the modulus, has been followed as a function of time at constant temperature, degree of deformation, and frequency.

At 50 °C, no change in G' is recorded as a function of time. At 46 °C an increase of G' as a function of time is observed (Figure 13). At this temperature, only a very small fraction of units have adopted a regular helix conformation. This fraction can be obtained from Figure 2. A value of 100 Pa is reached after 40 min. Then the increase slows down and G' reaches a value of 1.7×10^3 Pa after several hours (Figure 14). Intermediate cooling of the solution to 40 °C accelerates the transformation. Once the plateau value is reached at 46 °C, the sample is cooled to 20 °C. This results in a rapid increase of the modulus almost within the time needed to reach the low temperature. Heating to 46 °C brings the modulus back to the plateau value, initially obtained at this temperature. No hysteresis is observed for this part of the modulus. An important hysteresis, however, is observed for that part of the modulus that results from the isothermal treatment at 46 °C. The decrease of this part of the modulus sets in above 50 °C.

2. Phase Behavior of sPMMA in Toluene. The concentration dependence of the different thermal transitions has been investigated by DSC, and the experimental data are brought together in Figure 15. Only a glass transition (T_g) is observed for polymer concentration $w_2 > 0.70$. It decreases with increasing solvent content. At lower polymer concentration, the exothermic and endothermic transition, already reported in the first part, takes place up to very low concentration. The temperature at the onset of the exotherm (T_{gel}) and at the end of the endotherm (T_m) are plotted in Figure 15 as a function of the polymer concentration. The concentration dependence of T_{gel} is ascribed to the dynamic nature of the experiment. The decrease of T_{gel} at the low polymer concentration side is ascribed to a decrease of the rate of gelation with decreasing polymer concentration. At constant scanning rate this manifests itself as a decrease of T_{gel}.

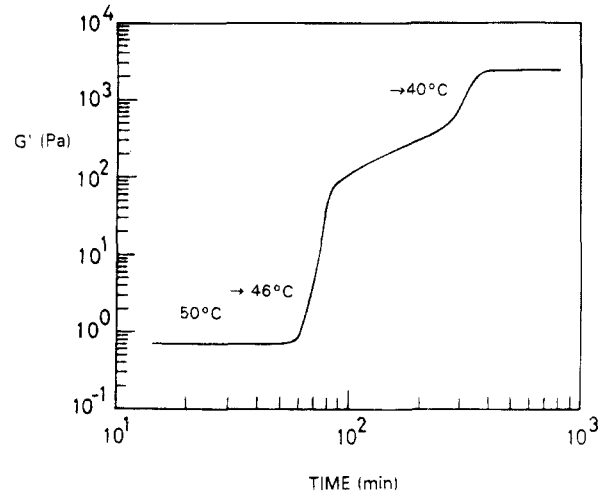

Figure 13. Time dependence of G' at different temperatures (sPMMA1 in toluene; $w_2 = 0.1$).

The melting point of the gel, T_m, increases with increasing the w_2. These melting points have only be reported up to $w_2 \approx 0.70$. At higher polymer concentrations, only very small endothermic signals have been observed with some samples, and no reproducible melting points could be deduced. Extrapolation to $w_2 = 1.00$ leads to a melting point that is lower than the T_g of the solvent free polymer.

3. Gelation mechanism. The combination of the data obtained with different experimental techniques provides firm evidence for the two step mechanism already reported in a previous paper for solutions of sPMMA in *o*-xylene.[18] A fast change in intramolecular conformation takes place in a narrow temperature region. It is associated with an important decrease of molecular mobility and an expansion of the chain. This last phenomenon is reflected in the increased interaction of the pendant groups with the solvent which is less polar than the polymer chain units. This change in chain conformation is followed by an intermolecular association.

Distinction between these two steps can only be made at high temperature at which only a small fraction of chain units have adopted a helix conformation. At these temperatures, the intramolecular transformation as observed by IR is still very fast. The intermolecular association on the contrary, reflected by the time dependence of G', extends over a period of several hours. This time dependence of intermolecular association is also illustrated by the light scattering data. The slow step is a kinetic second-order transition at high temperature and leads to the formation of the gel network,

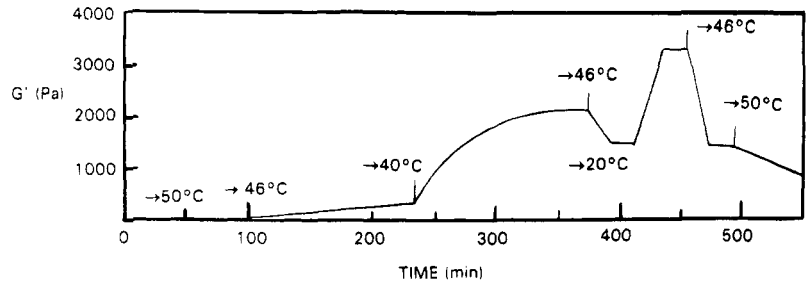

Figure 14. Time and temperature dependence of G' (sPMMA1; $w_2 = 0.1$).

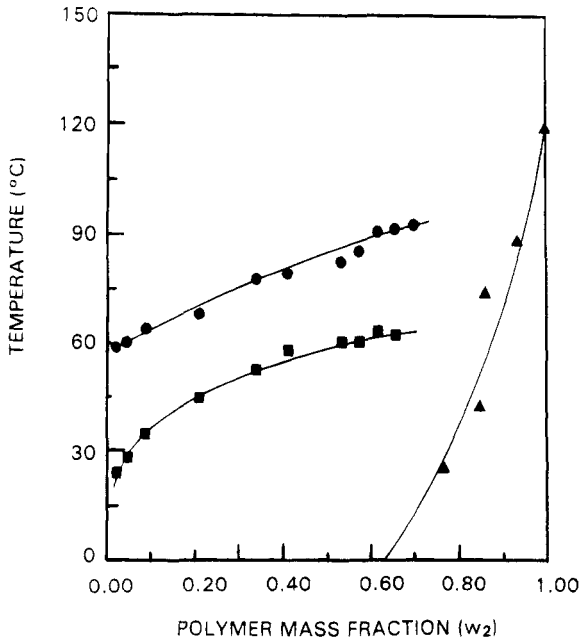

Figure 15. Phase diagram of the system sPMMA–toluene (●, melting temperature; ■, gelation temperature; ▲, glass transition temperature).

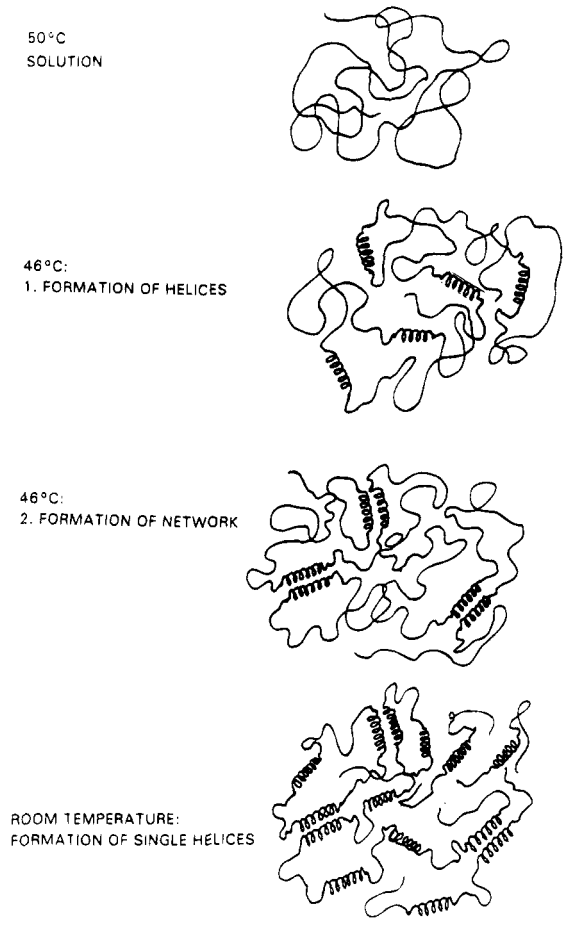

Figure 16. Schematic representation of the gelation mechanism.

or, at low polymer concentration to the formation of micro gel particles. At low temperature, gelation proceeds much faster and no quantitative kinetic analysis can be made. The kinetic data do not allow us to distinguish between the formation of a simple or double helix. But the formation of a double helix is not necessary to lead to the continuity of a three-dimensional network.

Another interesting observation is the occurrence of two different rheological transitions. The physical network, formed only by a small fraction of helix segments after isothermal annealing at 46 °C, melts far above its formation temperature. Cooling to room temperature after this isothermal annealing transforms most of the remaining chain segments into helices. This results in an increase of the stiffness of the system and is reflected in a further increase of G'. Heating of the system to 46 °C restores the G' value, obtained after isothermal annealing at that temperature. The structures formed by cooling therefore melt without hysteresis, and one can conclude that single-helix segments are formed that do not agglomerate into supramolecular structures. They therefore melt at their formation temperature. The different steps are illustrated in Figure 16.

Annealing at high temperature results in a physical network with low cross-linking density. Once this network is formed, it will be kept expanded by the osmotic pressure exerted by the solvent. Cooling results in an increase of the number of chain segments with a helix conformation. They have less tendency to agglomerate because of this osmotic force.

This mechanism of structure formation is therefore different from the "normal" crystallization. During this "normal" crystallization, the gain in free energy is realized in one step as both the intramolecular and intermolecular step occur simultaneously. The change in molecular conformation takes place during the formation of the crystal, and the helix gets its stability from its incorporation in the crystal lattice.

In the two-step gelation mechanism, an important gain in energy is already realized in the first step which is the intramolecular change in conformation. The gain in energy in the second step, the intermolecular association, is therefore less important. This two-step decrease of the free energy also explains the peculiar rheological behavior reported in Figure 13. At high temperature, a limited number of chain segments will be transformed into a helix conformation. This low helix content will lead to the formation of a physical network with a low degree of cross-linking. When this network is cooled to room temperature, most of the remaining

sequences will transform into helices and this will stiffen the network. But they will not associate anymore as the gain in energy by this second, intermolecular step will not be large enough to compete with the osmotic pressure exerted by the solvent in the swollen, physical network. These nonassociated helices will "melt" without hysteresis. The helices agglomerated during the high temperature treatment will melt with a certain degree of hysteresis.

Conclusions

The thermoreversible gelation of solutions of sPMMA in toluene follows the mechanism proposed earlier for solutions of sPMMA in *o*-xylene. A two-step structure formation takes place. A fast intramolecular change from a coil to a helix conformation is followed by a slower intermolecular association.

No firm evidence for the formation of a double helix can be found. The occurence of a two step gelation mechanism suggests rather the formation of a single helix. The formation of double helices in the first step would lead to a much faster intermolecular network formation as the physical cross-links could be formed already at the first step of the process, the conformational change. This should lead to a much faster increase of G' with time, and this change should parallel the change in molecular conformation.

Acknowledgment. The authors thank the ministry of "Wetenschapsbeleid-DWTC" for financial support through IUAP-III-040 and IUAP-II-16. The FKFO, FGWO, and DSM are thanked for continuous support to the laboratory. S.T. thanks the IWONL for a doctoral fellowship. M.B. and M.C. thank DSM for a doctoral fellowship.

References and Notes

(1) Spěváček, J.; Schneider, B. *Adv. Colloid Interface Sci.* **1987**, *27*, 81.
(2) Könnecke, K.; Rehage, G. *Colloid Polym. Sci.* **1981**, *259*, 1062.
(3) Könnecke, K.; Rehage, G. *Makromol. Chem.* **1983**, *184*, 2679.
(4) Rehage, G. *Colloid Polym. Sci.* **1975**, *57*, 7.
(5) Spěváček, J. *J. Polym. Sci., Polym. Phys.* **1978**, *16*, 523.
(6) Spěváček, J.; Schneider, B. *Polym. Bul.* **1980**, *2*, 227.
(7) Spěváček, J.; Schneider, B.; Bohdanecky, M.; Sikora, A. *J. Polym. Sci., Polym. Phys.* **1982**, *20*, 1623.
(8) Mrkvičková, L.; Stejskal, J.; Spěváček, J.; Horská, J.; Baldrian, J. ; Quadrat, O. *Polymer* **1983**, *24*, 700.
(9) Sedláček, B.; Spěváček, J.; Mrkvičková, L.; Stejskal, J.; Horská, J.; Baldrian, J.; Quadrat, O. *Macromolecules* **1984**, *17*, 825.
(10) Spěváček, J.; Schneider, B. *Polym. Lett. Ed.* **1974**, *12*, 349.
(11) Spěváček, J.; Schneider, B. *Makromol. Chem.* **1975**, *167*, 3409.
(12) Spěváček, J.; Schneider, B. *Polymer* **1978**, *19*, 63.
(13) Dybal, J.; Stokr, J.; Schneider, B. *Polymer* **1983**, *24*, 971.
(14) Spěváček, J.; Schneider, B.; Baldrian, J.; Dybal, J.; Stokr, J. *Polym. Bull.* **1983**, *9*, 495.
(15) Spěváček, J.; Schneider, B.; Dybal, J.; Stokr, J.; Baldrian, J.; Pelzbauer, Z. *J. Polym. Sci. Polym. Phys.* **1984**, *22*, 617.
(16) Kusuyama, H.; Takase, M.; Higashihata, Y.; Tseng, H. T.; Chatani, Y. T.; Tadokoro, H. *Polymer* **1982**, *23*, 1256.
(17) Kusuyama, H.; Miyamoto, N.; Chatani, Y. T.; Tadokoro, H. *Polymer* **1983**, *14*, 1256.
(18) Berghmans, H.; Donkers, A.; Frenay, L.; Stoks, W.; De Schryver, F. C.; Moldenaers, P.; Mewis, J. *Polymer* **1987**, *28*, 97.
(19) Randal, J. C. *Polymer Sequence Determination*; Academic Press: New York, 1977.
(20) Holden, D. A.; Wang, P. Y. K.; Guillet, J. E. *Macromolecules* **1980**, *13*, 295.
(21) Khalil, M. M. H.; Boens, N.; Van der Auweraer, M.; Ameloot, M.; Andriessen, R.; Hofkens, J.; De Schryver, F. C. *J. Phys.Chem.* **1991**, *95*, 9375.
(22) Chu, D.-Y.; Thomas, J. K. *Macromolecules* **1984**, *17*, 2142.
(23) Dybal, J.; Spěváček, J.; Schneider, B. *J. Polym. Sci. Polym. Phys.* **1986**, *24*, 657.
(24) Spěváček, J. *Makromol. Chem., Makromol. Symp.* **1990**, *39*, 71.
(25) Berghmans, M.; Govaers, S.; Berghmans, H.; De Schryver, F. C. *Polym. Eng. Sci.* **1992**, *32*, 1466.
(26) Berghmans, M.; Govaers, S.; De Schryver, F. C.; Berghmans, H. *Chem. Phys. Lett.* **1993**, *205*, 140.